

RHDE models in FRW Universe with two IR cut-offs with redshift parametrization

Archana Dixit¹, Vinod Kumar Bhardwaj² Anirudh Pradhan³

^{1,2,3}Department of Mathematics, Institute of Applied Sciences and Humanities, GLA University, Mathura, Uttar Pradesh-281 406, India

¹E-mail: archana.dixit@gla.ac.in.

²E-mail: dr.vinodbhardwaj@gmail.com, vinod.bharadwaj@gla.ac.in

³E-mail: pradhan.anirudh@gmail.com

Abstract

In this manuscript, we have researched the cosmic expansion phenomenon in flat FRW Universe through the interaction of the recently proposed R enyi holographic dark energy (RHDE). For this reason, we assumed Hubble (H) and Granda–Oliveros (GO) horizons as IR cut-off in the framework of $f(R, T)$ gravity. With this choice for IR cut-off, we can obtain some important cosmological quantities such as the equation of state ω_T , energy density ρ_T , density parameter Ω_T , and pressure p_T , which are the function of the redshift z . It is observed that in both IR cut-offs the EoS parameter displays quintom-like behaviour for three different values of δ . Here we plot these parameters versus redshift z and discuss the consistency of the recent findings. Next, we explore the ω_T - ω'_T plane and the stability analysis of the dark energy model by a perturbation method. Our findings demonstrate that the Universe is an accelerating model of rapid growth that is explained by quintom like behaviour. Hence the feasibility of the RHDE model with Hubble and GO cut-off is supported by our model. The results indicate that the IR cut-offs play a significant role in the understanding of the dynamics of the universe.

Keywords :FRW universe, RHDE, Hubble horizon, GO- horizon.

PACS: 98.80.-k, 98.80.Jk, 04.20.Jb

1 Introduction

Observational information received by (SNIa) [1]- [2], large scale structures (LSS) [3]- [5] and cosmic microwave background (CMB), anisotropies [6]- [7] confirmed the present accelerated expansion of the universe. The dark energy is assumed as a responsible candidate for this present scenario of accelerated Universe [8]- [10]. The character of DE is unknown, and mysterious. The easiest choice for DE is cosmological constant with positive energy density and negative pressure.

The cosmological constant faces several challenges, such as the issue of fine tuning, and the problem of coincidence [8]. One reasonable way of relieving the question of cosmic coincidence is to assume that dark matter (DM) and dark energy (DE) interact. For the complex DE scenario, there are different alternate theories suggested by observing the accelerating universe:

(a) the scalar-field models of DE including quintessence [11], tachyon [12], k-essence [13], (b) the interacting DE models including chaplygin gas [14], polytropic gas [15]- [16], phantom [17] and holographic dark energy (HDE) [18]- [19]. On the other hand, the nature of DE can be investigated on the basis of certain principles of quantum gravity, which would be the yield to the (HDE) model [20]- [24].

Another approach to solving the dark energy problem is to connected the certain aspects of the theory of quantum gravity, known as the holographic principle [25]- [28]. Several authors are focusing on the numerous cosmological implications of new and modified HDE models [29]- [33]. Another significant factor of this model is the IR cut-off. A lot of HDE models are discussed in the literature, depending on the IR cut-off.

Many authors are working on the different IR cut-offs like: Sharma and Dubey [34] worked on the interacting R nyi holographic dark energy with parametrization on the interaction term and studied the graphical behaviour of cosmological parameters. Vipin et al. [35] have also observed the growth rate of perturbations by using hierarchy. The anisotropic and spatially homogeneous Bianchi type- VI_0 (RHDE) models of general relativity discussed in [36]. In this model authors assumed both (H) and (GO) horizons as IR cut-off and obtained cosmological parameters. In the same context, Tayeb *et al.* [37] analysed the anisotropic R nyi holographic dark energy models in flat space-time. Qolibikloo and Ghodsib [38] investigate the R nyi entropy and inequalities under the phase transition. The expansion and growth data were combined by Akhlaghi [39] to investigate the ability of the three most popular HDE models, namely the Ricci scale, future event horizon, and Granda–Oliveros IR cut-offs.

In this sequence, Ghaffari [40] examined the cosmological models of HDE in a DGP braneworld with GO cut-off. In recent year many entropy formalisms has been used and explore the cosmological models. Some new HDE models are being developed, such as the RHDE model, [41], Sharma–Mittal HDE (SMHDE) [42] and Tsallis HDE (THDE). Among these models RHDE is more stable model which is based on non-interactions between cosmic region [43]- [44]. Younas *et al.* [45] have investigated entropies of R nyi, Tsallis and Sharma–Mittal in flat FRW Universe within Chern–Simons modified gravity. HDE model was conjectured as IR cut-off with Benkenstein entropy and Hubble horizon that does not provide an appropriate explanation for the level of a flat FRW universe [46]- [48]. Recently, a new HDE model was proposed and explored by changing the standard HDE as $S_\delta = \gamma A_r^\delta$, where γ is an unspecified constant $A_r = 4\pi L^2$ represents the area of the horizon and δ is a non-additivity parameter, called Tsallis holographic dark energy (THDE) [44, 49]. Another possibility for DE showed up when Cohen *et al.* [50] applied some speculation on the mutual connection between UV (Λ) and IR (L) cut-offs and the entropy of framework, expressing as $\rho_\Lambda \propto \frac{S}{L^4}$. where ρ_Λ is the vacuum energy density [50]. Bekenstein and Hawking [51, 52] studied the thermodynamics of the black hole. It is indicated that the Bekenstein–Hawking entropy bound $S_{BH} \sim M_p^2 L^2$, scales as the region $A_r \sim L^2$ rather than the volume $V \sim L^3$ and M_p is the reduced Plank mass ($8\pi G = 1/M_p^2 = 1$). On the other hand, the Bekenstein entropy bound S_B is EL for the case where $E = \rho_\Lambda L^3$ is the energy, and L is the IR cut-off. For $\rho_\Lambda \leq M_p^2 L^{-2}$ by using $S_B < S_{BH}$. Here C_1^2 is a numerical constant, given the HDE:

$$\rho_d = 3C_1^2 M_p^2 L^{-2}. \quad (1)$$

Observational information, which is acquired by restricting the HDE model, clearly demonstrate $C_1 = 0.818^{+0.113}_{-0.097}$ [53] and $C_1 = 0.815^{+0.179}_{-0.039}$ [54] for flat and non-flat space time separately. Several research on the HDE model and its features are reported in [55]- [58]. The two latest entropies R nyi and Tsallis [59]- [62] are commonly used to study various gravitational and cosmological phenomena [63]- [71]. HDE density derivation is based on the relationship of entropy-area $S_{BH} = A_r/4$, where A_r is the area of black hole horizon. Subsequently, by changing the entropy relation, one can locate new type of HDE. It is surprising that the form of HDE and gravity model equations can be generalized by using a generalized method of entropy-area relationship. So, we have a generalized Friedmann equation to define evolution of the universe. This idea motivates us to look through R nyi entropy into the constructive accelerating phases of the Universe. The entropy in RHDE was discussed in Refs. [65]- [67].

$$S_R = \frac{1}{\delta} \ln(1 + \delta S_T). \quad (2)$$

Here δ is a constant and S_T is Tsallis entropy. Bekenstein and Tsallis is equal [65–67, 71] then Eq. (2) becomes:

$$S_R = \frac{1}{\delta} \ln(1 + \delta \frac{A_r}{4}), \quad (3)$$

if δ tends to zero, the R nyi entropy reduces to $A_r/4$. During the current work, we are considering HDE by applying the R nyi entropy. In this direction a brief survey of the theories of modified gravity as the new participation explored a cosmological reconstruction. Harko *et al.* [72] developed new generalized theory known as $F(R, T)$ gravity.

Several cosmologist [73]- [75] have studied $f(R, T)$ gravity in distinct context. The main aim of our proposed model is to consider $f(R, T)$ model with R nyi HDE by assuming two IR cut-offs. The work in this manuscript is configured as: The field equations of $f(R, T)$ gravity is set out in Sect.2. R nyi HDE models are considered in Sect.3. R nyi HDE model with Hubble horizon cut-off are discussed in Sect.3.1. R nyi HDE model with GO horizon cut-off is examined in Sect.3.2. $\omega_T - \omega'_T$ plane is discussed in Sect.4. The stability of the model is discussed in Sect.5 and the outcomes are summarized with conclusions that are discussed in Sect.6.

2 Basic field equations of f(R,T) gravity

We assume that the behaviour for the modified gravity theories takes the form:

$$\mathbb{S} = \frac{1}{16\pi} \int f(R, T) \sqrt{-g} d^4x + \int L_m \sqrt{-g} d^4x. \quad (4)$$

Here $f(R, T)$ is an arbitrary function of the trace (T) and Ricci scalar (R). Here L_m is the matter Lagrangian density.

The stress-energy tensor of matter is defined as [76]

$$T_{ij} = -\frac{2}{\sqrt{-g}} \frac{\delta(\sqrt{-g} L_m)}{\delta g^{ij}}. \quad (5)$$

The field equations of the $F(R, T)$ model are obtained as

$$2F_R(R, T)R_{ij} - F(R, T)g_{ij} + 2(g_{ij}\square - \nabla_i \nabla_j)f_R(R, T) = 16\pi T_{ij} - 2F_T(R, T)T_{ij} - 2F_T(R, T)\Theta_{ij}. \quad (6)$$

However, the stress-energy tensor for the current work is considered as

$$T_{ij} = -pg_{ij} + (p + \rho)u_i u_j. \quad (7)$$

Also, the matter Lagrangian can be assumed as $L_m = -p$. The conditions $u_i u^i = 1$ and $u^i \nabla_j u_i = 0$ satisfy the four-velocity. In our model, we assumed the particular case of $f(R, T)$ expressing by the function $f(R, T) = 2f(T) + R$, where $f(T)$ is an arbitrary function of the stress-energy tensor of matter. The gravitational field equations follows by Eq. (6) written as

$$2R_{ij} - Rg_{ij} = 16\pi T_{ij} + 4\dot{f}(T)T_{ij} + 2[2p\dot{f}(T) + f(T)]g_{ij}, \quad (8)$$

where the dot indicates the derivative is related to the argument. For the dust filled universe ($p = 0$), the gravitational field equations are given by

$$2R_{ij} - Rg_{ij} = 16\pi T_{ij} + 4\dot{f}(T)T_{ij} + 2f(T)g_{ij}. \quad (9)$$

These field equations are suggested in [77]. We can obtain a cosmological model by considering the dust Universe, by select the function $f(T) = \xi T$, $\xi \rightarrow \text{constant}$.

The metric of a flat FRW Universe is considered as:

$$ds^2 = dt^2 - a^2 (dx^2 + dy^2 + dz^2). \quad (10)$$

The gravitational field equations are written as,

$$3 \left(\frac{\dot{a}^2}{a^2} \right) = (8\pi + 3\xi)\rho_T, \quad (11)$$

$$2\frac{\ddot{a}}{a} + \frac{\dot{a}^2}{a^2} = \xi\rho_T. \quad (12)$$

This $f(R, T)$ gravitational model is equal to efficient cosmological constant $\Lambda_{eff} \propto H^2$, where $H = \frac{\dot{a}}{a}$ is the Hubble function [77]. Field equations are reduced in terms of H ,

$$2\dot{H} + 3\frac{8\pi + 2\xi}{8\pi + 3\xi}H^2 = 0. \quad (13)$$

The general solution of the above Eq. (13) obtained as

$$H(t) = \frac{2}{3t} \frac{(8\pi + 3\xi)}{(8\pi + 2\xi)} = \frac{2\beta}{3t}, \quad (14)$$

where $\mathbf{a}(\mathbf{t}) = \mathbf{t}^{\frac{2}{3}\beta}$ is the scale factor where $\beta = \frac{(8\pi+3\xi)}{(8\pi+2\xi)}$.

Here we are using different expression for H , like future event Hubble horizon as the infrared cut-off, Ref. [78] and GO infrared cut-off. By the conservation equation we obtained as

$$\frac{\partial \rho_T}{\partial t} + 3H(\rho_T + p_T) = 0. \quad (15)$$

Here ρ_T is the R enyi holographic energy density, solving Eq.(15) the EoS parameter ω_T can be rewrite as:

$$\omega_T = -1 - \frac{1}{3H} \left(\frac{\dot{\rho}_T}{\rho_T} \right). \quad (16)$$

3 R nyi HDE model

We have taken a system with m , states with P_i probability distribution and satisfies the condition $\sum_{i=1}^m P_i = 1$. R nyi and Tsallis entropy are well known parameter of generalized entropy [49].

$$S_R = \frac{1}{\delta} \ln \sum_i^m P_i^{1-\delta} \quad S_T = \frac{1}{\delta} \ln \sum_{i=1}^m P_i^{1-\delta} - P_i, \quad (17)$$

where $\delta = 1 - U$ and U is a real parameter. Now using the above equations we get the relation,

$$S_R = \frac{1}{\delta} \ln(1 + \delta S_T). \quad (18)$$

In Eq. (18) the Bekenstein entropy is $S_T = \frac{A_r}{4}$, and $A_r = 4\pi L^2$. This gives the R nyi entropy of the system as $S_R = \frac{1}{\delta} \ln(1 + \delta \pi L^2)$ [60].

In this section we take the assumption $\rho_T dV \propto T ds$ [69] then we can get the R nyi HDE density in IR cut-off written as

$$\rho_T = \frac{3C_1^2}{8\pi L^2} \frac{1}{(1 + \pi \delta L^2)}. \quad (19)$$

In this case, C_1^2 is the numerical constant, V is the volume, and T is the temperature of the system. We have used $T = \frac{H}{2\pi}$ and $A = \frac{4\pi}{H^2} = 4\pi(\frac{3V}{4\pi})^{2/3}$, relationships valid for the flat FRW Universe. It is clear that we have $\rho_T = \frac{3C_1^2 H^2}{8\pi}$ is a complete agreement with OHDE [21, 46, 47] in the absence of δ . In this section, we use the R nyi entropy by considering the Bekenstein entropy as the Tsallis entropy [63]- [69].

Finally, we are proposing a new holographic dark energy model, which is RHDE. Next we have examined the well-known cosmological parameters of H and GO IR cut-off in Sect.3.1 & Sect.3.2.

3.1 Model-I: R nyi HDE model with hubble horizon cut-off with redshift parameterization

Hubble horizon is the simplest choice with the Hubble length $L = H^{-1}$ [48]. According to the holographic principle the energy density of DE is proportional to the square of the Hubble parameter i.e., $\rho_T \propto H^2$ [39]. The principle states that the given choice can solve the fine tuning problem.

Here the R nyi energy density is obtained as

$$\rho_T = \frac{3C_1^2 H^2}{8\pi} \left(1 + \frac{\pi \delta}{H^2}\right)^{-1} \quad (20)$$

Utilizing Hubble horizon as a possibility for IR cut-off i.e., $L = \frac{1}{H}$ and $8\pi = 1$. In this analysis we use the $a = \frac{a_0}{(1+z)}$ redshift parameterization,

$$\rho_T = \frac{2\beta^4 C_1^2}{12\pi \beta^2 \left(\frac{a_0}{z+1}\right)^{3/\beta} + 27\pi^2 \delta \left(\frac{a_0}{z+1}\right)^{6/\beta}}. \quad (21)$$

By using Eqs.(16) and (21), we get EoS parameter defined as,

$$\omega_T = \frac{-9\pi\beta\delta\left(\frac{a_0}{z+1}\right)^{3/\beta} + 18\pi\delta\left(\frac{a_0}{z+1}\right)^{3/\beta} - 4\beta^3 + 4\beta^2}{9\pi\beta\delta\left(\frac{a_0}{z+1}\right)^{3/\beta} + 4\beta^3}. \quad (22)$$

By using Eqs.(21) and (22) we get pressure as,

$$p_T = -\frac{2\beta^3c^2\left(9\pi\beta\delta\left(\frac{a_0}{z+1}\right)^{3/\beta} - 18\pi\delta\left(\frac{a_0}{z+1}\right)^{3/\beta} + 4\beta^3 - 4\beta^2\right)}{3\pi\left(4\beta^2\left(\frac{a_0}{z+1}\right)^{\frac{3}{2\beta}} + 9\pi\delta\left(\frac{a_0}{z+1}\right)^{\frac{9}{2\beta}}\right)^2}. \quad (23)$$

Using Eqs.(14) and (21), we obtain density parameter as

$$\Omega_T = \frac{\beta^2C_1^2}{18\pi^2\delta\left(\frac{a_0}{z+1}\right)^{3/\beta} + 8\pi\beta^2}. \quad (24)$$

The behaviour of cosmological parameters such as energy density, Eos parameter, pressure and density parameter are shown in this section, where the density parameter Ω_T is defined as the ratio between the actual (or observed) density ρ_T and the critical density ρ_c of the Friedmann Universe. Here $\rho_c = \frac{3H^2}{8\pi}$, the relation between the actual density and the critical density determines the overall geometry of the Universe; when they are equal, the geometry of the Universe is flat (Euclidean) of the total RHDE in IR cut-off.

3.2 Model-II: R enyi HDE model with Granda–Oliveros (GO) horizon cut-off with redshift parameterization

Granda and Oliveros first [79, 80] introduced the cut-off $L = (kH^2 + m\dot{H})^{-1/2}$ and attempt to resolve the well known cosmological problems like cosmic coincidence and stability. In this sequence, the acceleration combined the Hubble parameter together with its time derivative. On substituting GO cut-off in Eq. (14) and taking ($8\pi = 1$), we get $L = \frac{1}{\frac{4}{9}\beta^2k\left(\frac{a_0}{z+1}\right)^{-3/\beta} - \frac{2}{3}\beta m\left(\frac{a_0}{z+1}\right)^{-3/\beta}}$.

By using Eq. (20), we get energy density as,

$$\rho_T = \frac{2\beta^4c^2\left(\frac{a_0}{z+1}\right)^{-6/\beta}(3m - 2\beta k)^4}{27\pi\left(81\pi\delta\left(\frac{a_0}{z+1}\right)^{6/\beta} + 16\beta^4k^2 - 48\beta^3km + 36\beta^2m^2\right)}. \quad (25)$$

By using Eqs. (16) and (25), we get EoS parameter defined as

$$\omega_T = \frac{-81\pi(\beta - 4)\delta\left(\frac{a_0}{z+1}\right)^{6/\beta} - 16(\beta - 2)\beta^4k^2 + 48(\beta - 2)\beta^3km - 36(\beta - 2)\beta^2m^2}{81\pi\beta\delta\left(\frac{a_0}{z+1}\right)^{6/\beta} + 16\beta^5k^2 - 48\beta^4km + 36\beta^3m^2}. \quad (26)$$

By using Eqs.(25) and (26) we obtained pressure as

$$p_T = \frac{2\beta^3c^2\left(\frac{a_0}{z+1}\right)^{-6/\beta}(3m - 2\beta k)^4\left(-81\pi(\beta - 4)\delta\left(\frac{a_0}{z+1}\right)^{6/\beta} - 4(\beta - 2)\beta^2(3m - 2\beta k)^2\right)}{27\pi\left(81\pi\delta\left(\frac{a_0}{z+1}\right)^{6/\beta} + 4\beta^2(3m - 2\beta k)^2\right)^2}. \quad (27)$$

Using Eqs.(14) and (25) we get density parameter as

$$\Omega_T = \frac{\beta^2 c^2 \left(\frac{a_0}{z+1}\right)^{-3/\beta} (3m - 2\beta k)^4}{18\pi \left(81\pi\delta \left(\frac{a_0}{z+1}\right)^{6/\beta} + 16\beta^4 k^2 - 48\beta^3 km + 36\beta^2 m^2\right)}. \quad (28)$$

Here we also calculate the well known cosmological parameters like energy density, Eos Parameter, pressure and density parameter Ω_T of the Friedmann Universe. We noticed that the geometry of the universe is flat (Euclidean) of the total RHDE in GO cut-off.

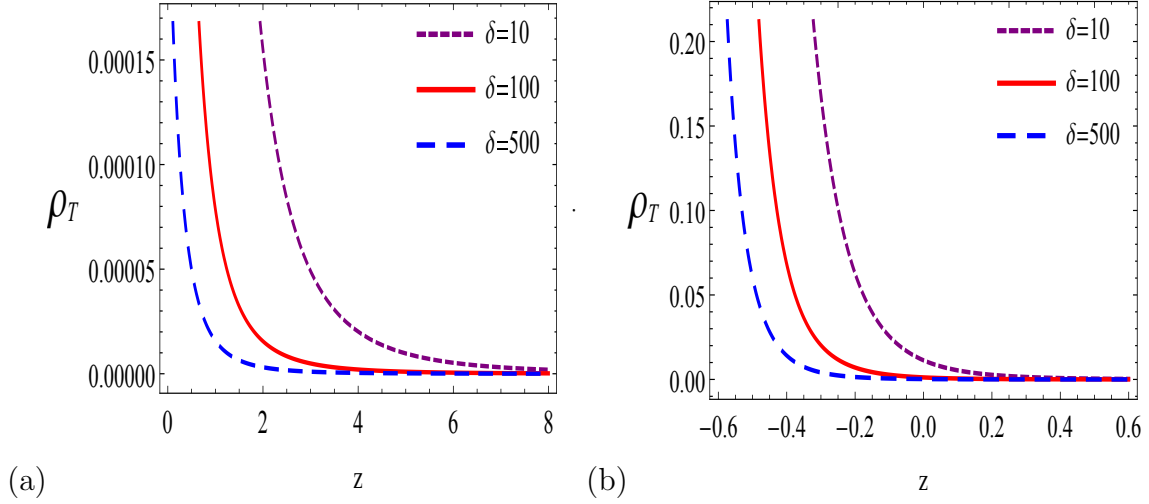


Figure 1: a. Plot of ρ_T versus z with (H hoz.) cut-off b. Plot of ρ_T versus z with (GO hoz.) cut-off

Figure 1a, b show the energy density of RHDE with Hubble horizon and GO horizon cut-off versus redshift z respectively. All the trajectories of ρ_T indicate the positive behaviour throughout the evolution of the universe for various estimations of δ . Likewise it can be seen that ρ_T is a positive decrease function and decreases, more sharply as δ increases. We observed RHDE is the decreasing function of redshift z in both IR cut-offs and we also found that in high redshift ρ_T tends to zero.

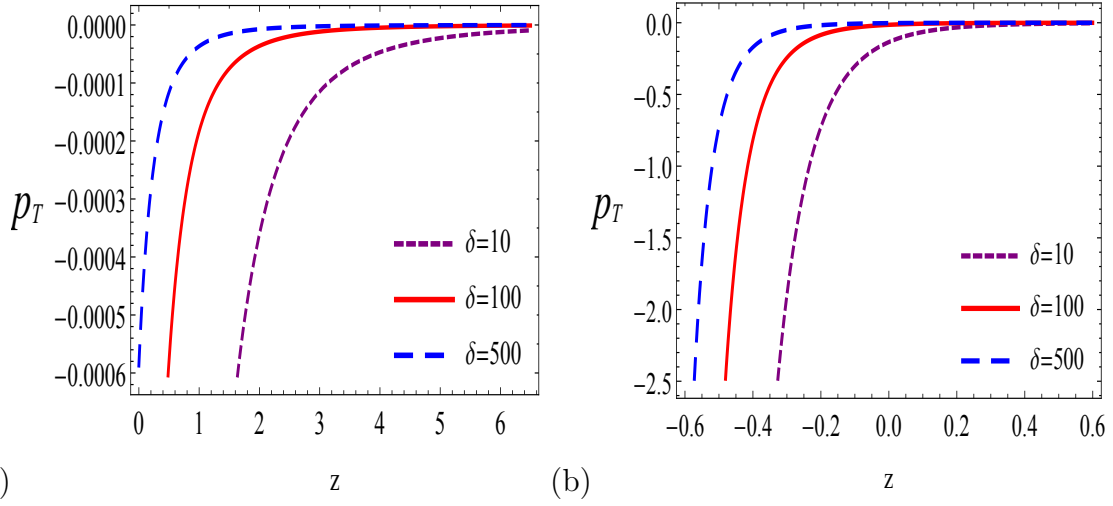


Figure 2: a. Plot of pressure p_T versus z (H hoz.) cut-off b. Plot of pressure p_T versus z (GO hoz.) cut-off

Figure 2a, b demonstrates the behaviour of pressure of RHDE with Hubble horizon and GO horizon cut-off versus redshift z respectively. Recent cosmological perceptions firmly show that our universe is dominated by the component with negative pressure called dark energy.

It is ascertained that the isotropic pressure is negative throughout the evolution. From the figures we noticed that the pressure is decreasing function of the redshift in both IR cut-offs.

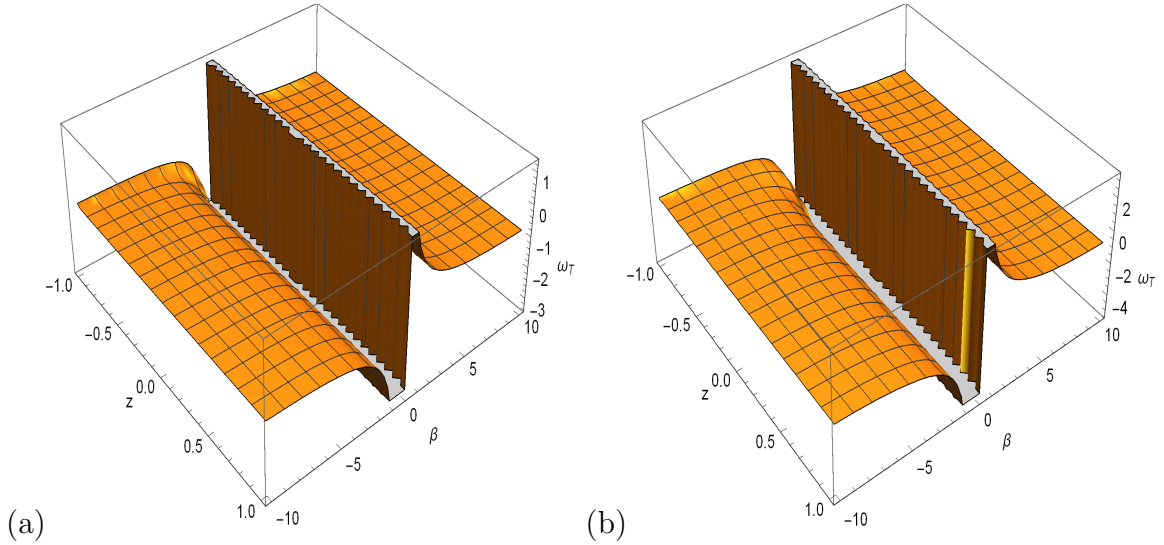


Figure 3: a. Plot of EoS parameter ω_T versus z (H hoz.) cut-off b. Plot of EoS parameter ω_T versus z (GO hoz.) cut-off

Table 1: The behaviour of EoS parameter ω_T with redshift parameterization for different values of β in Hubble Horizon cut-off

$\delta = 10$		$\delta = 100$		$\delta = 500$	
$\beta < 0$	Phantom	$\beta < 0$	Phantom	$\beta < 0$	Phantom
$0 < \beta \leq 1.88$	Quintessence	$0 < \beta \leq 1.98$	Quintessence	$0 < \beta \leq 1.99$	Quintessence
$1.88 < \beta \leq 2$	Quintessence \rightarrow Phantom	$1.98 < \beta \leq 2$	Quintessence \rightarrow Phantom	$1.99 < \beta \leq 10$	Quintessence \rightarrow Phantom
$2 < \beta \leq 10$	Phantom	$2 < \beta \leq 10$	Phantom	$2 < \beta \leq 10$	Phantom

Table 2: The behaviour of EoS parameter ω_T with redshift parameterization for different values of β in Granda–Oliver (GO) cut-off

$\delta = 10$		$\delta = 100$		$\delta = 500$	
$\beta < 0$	Phantom	$\beta < 0$	Phantom	$\beta < 0$	Phantom
$0 < \beta \leq 3$	Quintessence	$0 < \beta \leq 3.7$	Quintessence	$0 < \beta \leq 3.9$	Quintessence
$3 < \beta \leq 3.99$	quintessence \rightarrow Phantom	$3.7 < \beta \leq 3.99$	Quintessence \rightarrow Phantom	$3.90 < \beta \leq 4$	Quintessence \rightarrow Phantom
$4 < \beta \leq 10$	Phantom	$3.99 < \beta \leq 10$	Phantom	$4 < \beta \leq 10$	Phantom

Figure 3a implies that the EoS parameter ω_T is broadly used to categorize the different phases of the expanding universe. The EoS parameter of RHDE with H hoz. cut-off is given in Eq. (22). The mathematical analysis of Eos parameter regarding quintessence / phantom for different values of β in $[-10, 10]$ has been presented in Table 1 and 2 respectively. Here we notice that the EoS parameter initially lies in low phantom region or phantom era $\omega_T < -1$ at high redshift z and crossing the phantom divide line(PDL) $\omega_T = -1$. It enters in quintessence region and again lies in phantom region for different values of δ are shown in Table 1 and 2. Similarly in Figure 3b additionally demonstrations the analysis of the EoS parameter for the (RHDE-GO cut-off) which is shown in Eq. (26). In this figure we also observed that EoS parameter ω_T moves towards the high phantom region to quintessence region and after that again lies in phantom region for different values of δ . The trajectories of EoS parameter show the transition from phantom region to quintessence region by evolving the vacuum era of the universe in both IR cut-offs. This is called quintom-like nature of the universe.

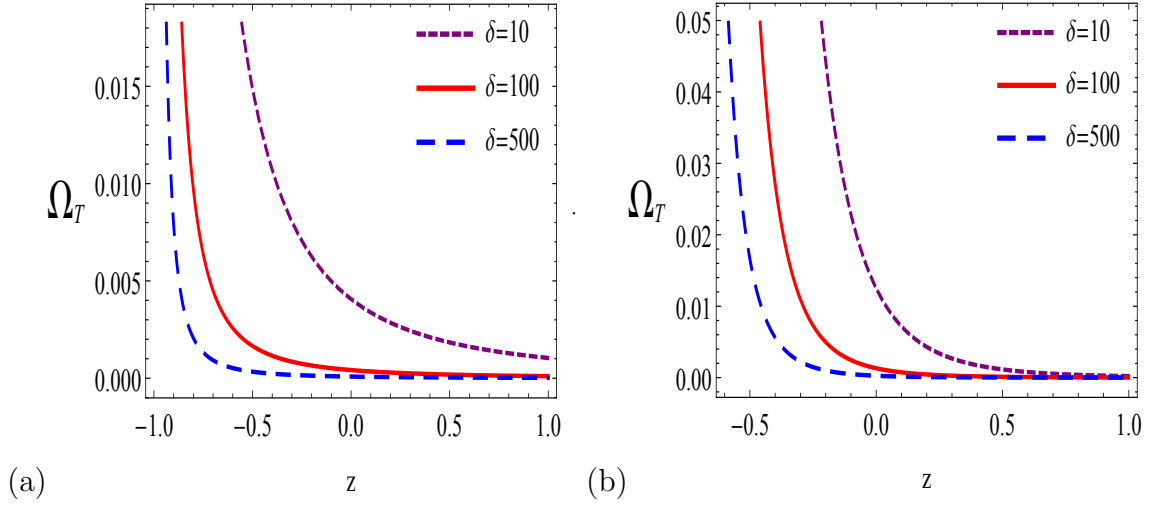


Figure 4: a. Plot of density parameter Ω_T versus z (H hoz.) cut-off b. Plot of density parameter Ω_T versus z (GO hoz.) cut-off.

Fig. 4 depicts the behaviour of density parameter Ω_T versus redshift z for various estimations of δ . In this figure the density parameter of the RHDE is seen to be lower region for the high redshift. We also noticed that the density parameter is positive throughout the evolution in both IR cut-offs.

4 Dynamics of ω_T - ω'_T plane

Caldwell and Linder [81, 82], recommend the ω_T - ω'_T plane to describe the dynamical property of DE model. Here ω_T is the EoS parameter and ω'_T is its evolutionary structure. Where dot means the derivative concerning $\ln a$. Here the $(\omega_T$ - ω'_T) plane was segregated in two regions, the thawing region $\omega_T < 0$, $\omega'_T > 0$ is the region where the EoS parameter evolves $\omega_T < -1$ increases with time and its evolution parameter shows positive behaviour, and the freezing region $\omega_T < 0$, $\omega'_T < 0$ in this region evolution parameter is negative.

For R enyi HDE with (H hoz.) IR-cut-off with redshift

We can obtain the ω'_T by differentiating the EoS parameter which is in Eqs. (22) and (26) with respect to $\ln a$ then we get

$$\omega'_T = \frac{d\omega_T}{d \ln a} = \frac{108\pi\delta \left(\frac{a_0}{z+1}\right)^{3/\beta}}{\left(9\pi\delta \left(\frac{a_0}{z+1}\right)^{3/\beta} + 4\beta^2\right)^2}. \quad (29)$$

For R enyi HDE with (GO hoz) IR cut-off with redshift

$$\omega'_T = \frac{d\omega_T}{d \ln a} = \frac{3888\pi\delta \left(\frac{a_0}{z+1}\right)^{6/\beta} (3m - 2\beta k)^2}{\left(81\pi\delta \left(\frac{a_0}{z+1}\right)^{6/\beta} + 16\beta^4 k^2 - 48\beta^3 km + 36\beta^2 m^2\right)^2}. \quad (30)$$

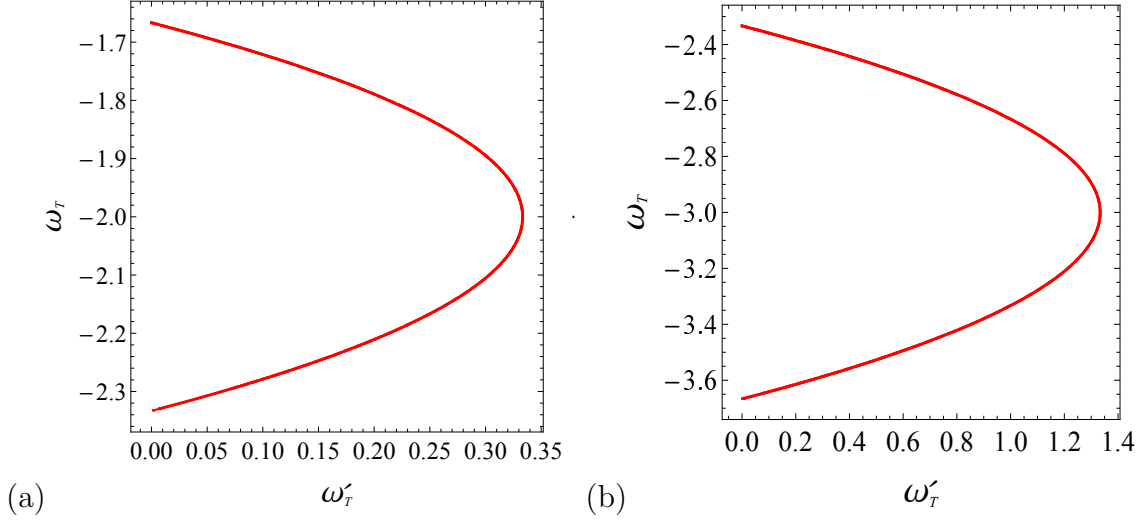


Figure 5: a. Plot of $\omega_T - \omega'_T$ versus z (H hoz) cut-off b. Plot of $\omega_T - \omega'_T$ versus z (GO hoz.) cut-off

From figure 5a, b we discuss the behaviour of $(\omega_T - \omega'_T)$ plane corresponding to Eqs. (29) and (30) for three different values of δ . These figures shows that $(\omega_T - \omega'_T)$ trajectories represents thawing region and are overlapped together during the whole evaluation.

5 Stability of the model

One may check the stability of the derived solution with respect to the perturbation of the space-time [83]- [84]. To this purpose, we considered the perturbations of volume scalar, directional Hubble factors and mean Hubble factor as

$$V \rightarrow V_B + V_B \sum_{i=1}^3 \delta b_i, \quad H_i \rightarrow H_{B_i} + \delta \dot{b}_i, \quad H \rightarrow H_B + \frac{1}{3} \sum_{i=1}^3 \delta \dot{b}_i, \quad \sum_{i=1}^3 H_i^2 \rightarrow \sum_{i=1}^3 H_{B_i}^2 + 2 \sum_{i=1}^3 H_{B_i} \delta b_i. \quad (31)$$

For metric perturbation δb_i to be linear the following equations must be satisfied

$$\sum_i \delta \ddot{b}_i + 2 \sum_i \theta_{B_i} \delta \dot{b}_i = 0, \quad (32)$$

$$\delta \ddot{b}_i + \frac{\dot{V}_B}{V_B} \delta \dot{b}_i + \sum_j \delta \dot{b}_j \theta_{B_i} = 0, \quad (33)$$

$$\sum \delta \dot{b}_i = 0. \quad (34)$$

From the simplification of above equations

$$\delta \ddot{b}_i + \frac{\dot{V}_B}{V_B} \delta \dot{b}_i = 0, \quad (35)$$

where the background volume scalar V_B leads to

$$V_B = t^{2\beta}. \quad (36)$$

From Eqs.(35) and (36), the metric perturbation becomes

$$\delta b_i = c_2 + c_1 \frac{t^{1-2\beta}}{(1-2\beta)}, \quad (37)$$

where c_1 and c_2 are constants of integration.

Thus, the actual fluctuation for each expansion factor $\delta a_i = a_{B_i} \delta b_i$ are expressed as

$$\delta a_i = c_2 t^{2\beta} + c_1 \frac{t}{(1-2\beta)}. \quad (38)$$

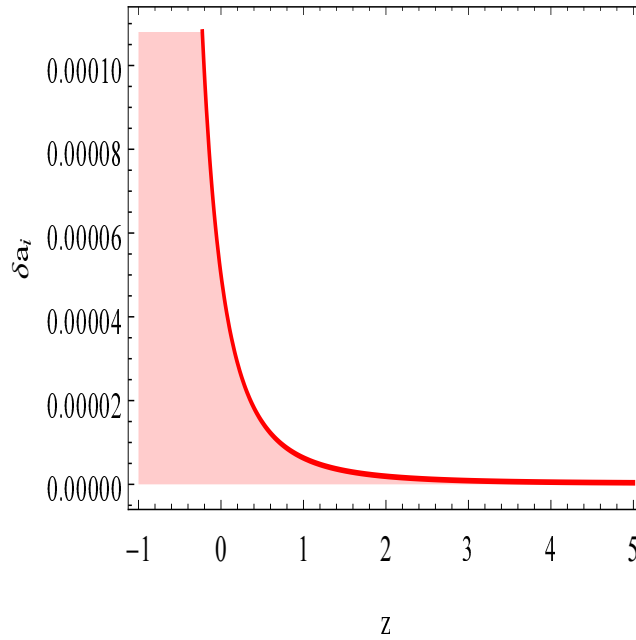


Figure 6: Plot of stability analysis with redshift z

From Eq.(38) and Fig. 6, we notice that the positive estimation of β , the δa_i approaches to zero for large $z \rightarrow \infty$ i.e. $\delta a_i \rightarrow 0$. Thus, the background solution is stable against the metric perturbation. This figure depicts the behaviour of actual fluctuations with respect to redshift. In past, the actual fluctuation is null but it increases minimally on later time.

6 Conclusion

In this work, the R enyi holographic type DE model with two IR cut-offs: Hubble horizon $L = \frac{1}{H}$ and Granda & Oliveros horizon $L = (kH^2 + m\dot{H})^{-1/2}$ cut-off have been discussed in $f(R, T)$ gravity by considering the parameters $k = 0.8$ and $m = 0.89$. For this purpose, we have analysed the cosmological features like: energy density, pressure, EoS parameter, density parameter, $(\omega_T - \omega'_T)$ plane and stability of the models are discussed. We have summarized our results as follows:

- The energy density of RHDE ρ_r is positive decreasing function for the three values of δ with redshift z . We found this behaviour is similar in both IR cut-offs as seen in Fig.1*a, b* respectively.
- Both models (I, II) indicate that the pressure is negative in all estimations throughout the evaluation seen in Fig.2*a, b*.
- The trajectories of EoS parameter show the transition from phantom region to quintessence region by evolving the vacuum era of the universe in both IR cut-offs as clear from Fig.3*a, b*.
- We also notice that the density parameter Ω_r is positive throughout the evolution in both IR cut-offs as seen in Fig.4*a, b*.
- The $(\omega_r - \omega_r')$ trajectories indicate the thawing region for the R nyi HDE model with Hubble horizon cut-off and GO cut-off as seen in Fig.5*a, b*.
- We have conducted that the perturbation analysis to examine the stability of the considered dark energy model and found that RHDE shows more stability during the comic evolution seen in (Fig.6). Subsequently our created model is stable.
- Here, we also include a comparative study of our work with recent works on this subject [34,35] and found that our findings are in good agreement with their work but their models are unstable whereas our both models are stable.

The feasibility of the R nyi holographic dark energy model with Hubble and GO cut-off is supported by our research and combined observational data is consistent with the future horizon.

Acknowledgments

The authors are heartily grateful to the anonymous referee for his constructive comments which improved the paper in the present form.

References

- [1] A.G. Riess *et al.*, Astron. J. **116**, 1009 (1998).
- [2] P.A. Bernardis *et al.*, Nature **404**, 955 2000.
- [3] M. Colless *et al.*, Mon. Not. R. Astron. Soc. **328**, 1039 (2001).
- [4] S. Cole *et al.*, Mon. Not. R. Astron. Soc. **362**, 505 (2005).
- [5] V. Springel, C.S. Frenk, Nature **440**, 1137 (2006).
- [6] S. Ade Hanany *et al.*, Astrophys. J. Lett. **545**, L5 (2000).
- [7] D.N. Spergel *et al.* Astrophys. J. Suppl. **148**, 175 (2003).
- [8] M. Roos, Wiley Chichester (2003).

- [9] S. Nojiri, S.D. Odintsov, Phys. Lett. B **639**, 144 (2006).
- [10] K. Bamba, S. Capozziello, S. Nojiri, S.D. Odintsov, Astrophys. Space Sci. **342**, 155 (2012).
- [11] M. Malekjani, T. Naderi, F. Pace, MNRAS **453**, 4148 (2015).
- [12] M.R. Setare, Phys. Lett. B **644**, 99 (2007).
- [13] T. Chiba, T. Okabe, M. Yamaguchi, Phys. Rev. D **62**, 023511 (2000).
- [14] V. Pasquier, U. Moschella, A.Y. Kamenshchick, U. Moschella, V. Pasquier, Phys. Lett. B **511**, 265 (2001).
- [15] K. Kleidis, N.K. Spyrou, Astron. Astrophys. **576**, A23 (2015).
- [16] K. Kleidis, N.K. Spyrou, Entropy **18**, 94 (2016).
- [17] S. Nojiri, S.D. Odintsov, Phys. Lett. B **562**, 147 (2003).
- [18] S. Weinberg, Rev. Mod. Phys. **61**, 1 (1998).
- [19] E.J. Copeland, M. Sami, S. Tsujikawa, Int. J. Mod. Phys. D **15**, 1753 (2006).
- [20] M.R. Setare, Chin. Phys. Lett. **26**, 029501 (2009).
- [21] S.D.H Hsu, Phys. Lett. B **594**, 13 (2004).
- [22] M.R. Setare, E.N. Saridakis, Phys. Lett. B **671**, 331 (2009).
- [23] M. Jamil, E.N. Saridakis, M.R. Setare, Phys. Lett. **679**, 172 (2009).
- [24] J. Lu, E.N. Saridakis, M.R. Setare, L. Xu, J. Cosmol. Astropart. Phys. **031**, 26 (2010).
- [25] J.D. Bekenstein, Phys. Rev. D **7**, 2333 (1973).
- [26] R. Bousso, JHEP **004**, 9907 (1999).
- [27] A. Cohen, D. Kaplan, A. Nelson, Phys. Rev. Lett. **82**, 4971 (1999).
- [28] L. Susskind, J. Math. Phys. (N.Y.) **36**, 6377 (1994).
- [29] D.R.K. Reddy *et al.*, Astrophys. Space Sci. **361**, 356 (2016).
- [30] Y. Aditya, D.R.K. Reddy, Eur. Phys. J. C **78**, 619 (2018).
- [31] V.U.M. Rao *et al.*, Results Phys. **10**, 469 (2018).
- [32] M.V. Santhi, *et al.*, Can. J. Phys. **95**, 381 (2017).
- [33] K.D. Naidu *et al.*, Eur. Phys. J. Plus **133**, 303 (2018).
- [34] U.K. Sharma, V.C. Dubey, arXiv:2001.02368, (2020).
- [35] V.C. Dubey, A.K. Mishra, U.K. Sharma, arXiv:2003.07883, (2020).
- [36] U.Y.D. Prasanthi, Y. Aditya, Results Phys. **17**, 103101 (2020).

- [37] T. Golanbari, K. Saaidi, P. Karimi, arXiv:2002.04097[astro-ph.CO] (2020).
- [38] S. Qolibiklooa, A. Ghodsib, Eur. Phys. J. C **79**, 406 (2019).
- [39] I.A. Akhlaghi *et al.*, MNRAS **477**, 3659 (2018).
- [40] S. Ghaffari, New Astron. **67**, 76 (2019).
- [41] H. Moradpour, *et al.*, Eur. Phys. J. C **78**, 829 (2018).
- [42] A.S. Jahromi, *et al.*, Phys. Lett. B **21**, 780 (2018).
- [43] M. Tavayef, A. Sheykhi, K. Bamba, H. Moradpour, Phys. Lett. B **781** 195 (2018).
- [44] C. Tsallis, L.J.L. Cirto, Eur. Phys. J. C **73**, 2487 (2013).
- [45] M. Younas *et al.*, Adv. High Energy Phys. **2019**, 1287932 (2019).
- [46] P. Horava, D. Minic, Phys. Rev. Lett. **85**, 1610 (2000).
- [47] S. Thomas, Phys. Rev. Lett. **89**, 081301 (2002).
- [48] L.N. Granda, A. Oliveros, Phy. Lett.B **671**, 199 (2009)
- [49] A. Jawad, K. Bamba, M. Younas, S. Qummer, S. Rani, Symmetry **10**, 635 (2018).
- [50] A.G. Cohen, D.B. Kaplan, A.E. Nelson, Phys. Rev. Lett. **82**, 4971 (1999).
- [51] J.D. Bekenstein, Phys. Rev. **D7** , 2333 (1973).
- [52] S.W. Hawking, Commun. Math. Phys. **43**, 199 (1975).
- [53] M. Li, X. D. Li, S. Wang, X. Zhang, J. Cosmol. Astropart. Phys. **2009**, 036 (2009).
- [54] M. Li, X. D. Li, S. Wang, Y. Wang, X. Zhang, J. Cosmol. Astropart. Phys. **2009**, 014 (2009)
- [55] B. Guberina, R. Horvat, H. Nikolic, J. Cosmol. Astropart. Phys. **2007**, 012 (2007).
- [56] S. Wang, Y. Wang, M. Li, Phys. Rep. **1**, 696 (2017).
- [57] B. Wang, E. Abdalla, F. Atrio-Barandela, D. Pavon, Rep. Prog. Phys. **79**, 096901 (2016)
- [58] K. karami, A. Abdolmaleki, N. Sahraei, S. Ghaffari, JHEP **150**, 1108 (2011).
- [59] C. Tsallis, Entropy **13**, 1765 (2011).
- [60] A. R enyi, Probability Theory (North-Holland, Amsterdam, 1970).
- [61] C. Tsallis, J. Stat. Phys. **52**, 479 (1988)
- [62] S. Nojiri, S.D. Odintsov and E.N. Saridakis, Eur. Phys. J. C **79**, 242 (2019)
- [63] A. Majhi, Phys. Lett. B **32**, 772 (2017).
- [64] A.S. Jahromi *et al.*, Phys. Lett. B **780**, 21 (2018).

- [65] N. Komatsu, Eur. Phys. J. C **77**, 229 (2017).
- [66] H. Moradpour, A. Bonilla, E.M.C. Abreu, J.A. Neto, Phys. Rev. D **96**, 123504 (2017).
- [67] H. Moradpour, A. Sheykhi, C. Corda, I.G. Salako, Phys. Lett. B **783**, 82 (2018).
- [68] H. Moradpour, Int. J. Theor. Phys. **55**, 4176 (2016).
- [69] H. Moradpour, et. al. Eur. Phys. J. C **78**, 829 (2018).
- [70] E.M. Barboza , R.C. Nunes, E.M.C. Abreu, J.A. Neto, Phys. A Stat. Mech. Appl. **436**, 301 (2015).
- [71] V.G. Czimmer, H. Iguchi, Phys. Lett. B **752**, 306 (2016)
- [72] T. Harko, Phys. Rev. D **81**, 044021 (2010).
- [73] S. Ram S.K Singh, M.K. Verma, Phys. Astron. Int. J. **4**, 330 (2018).
- [74] D.D. Pawar, R.V. Mapari, P.K. Agarwal, J. Astrophys. Astron. **40** 13 (2019).
- [75] P.K. Sahoo, P. Sahoo, B.K. Bishi, Int. J. Geom. Method Mod. Phys. **7**, 17 (2018).
- [76] L.D. Landau and E.M. Lifshitz, The Classical Theory of Fields, Butterworth-Heinemann, Oxford (1998).
- [77] N. J. Poplawski, arXiv:gr-qc/0608031.
- [78] V. Faraoni, Cosmology in Scalar-Tensor Theory, Kluwer Academic Publishers (2004).
- [79] S. Mizuno, S.J. Lee, E.J. Copeland, Phys. Rev. D **70**, 043525 (2004), astro-ph/ 0405490.
- [80] E.J. Copeland, M.R. Garousi, M. Sami, S. Tsujikawa, Phys. Rev. D **71**, (2005) 043003.
- [81] R.R. Caldwell, E.V. Linder, Phys. Rev. Lett. 2005, **95**, 141301–141304.
- [82] S. Bhattacharjee, arXiv:2006.04339v1[gr-qc] (2020).
- [83] L.K. Sharma, B.K. Singh, A.K. Yadav, Int. J. Geom. Method Mod. Phys., **1**, 2050111 (2020)
- [84] C.M. Chen, W.F. Kao, Phys. Rev. D **64** (2001) 124019.